Thesis for the Degree of Master of Science

Spin reorientation transition of ultrathin body-centered cubic Au/Ni(001)film

by

Jeonghwa Yang

Department of Physics

The Graduate School

Pukyong National University

Feburary 2009

Spin reorientation transition of ultrathin body-centered cubic Au/Ni(001)film

(BCC Au/Ni(001) 초박막에서의 스핀 방향 전이에 관한 연구)

Advisor : Jisang Hong

by

Jeonghwa Yang

A Thesis submitted in partial fulfillment of the requirements for the degree of Master of Science

in the Department of Physics, Graduate School,
Pukyong National University

Feburary 2009

Spin reorientation transition of ultrathin body-centered cubic Au/Ni(001)film

A dissertation

by

Jeonghwa Yang

Approved by:

Dr. Chanyong Hwang
Chair of Committee

Prof. Byung Kee Moon
Member of Committee

Prof. Jisang Hong
Member of Committee

Feburary 25, 2009

Content

List of Tables and Figures

Spin reorientation transition of ultrathin body-centered cubic Au/Ni(001)film

Jeonghwa Yang

Department of Physics, Graduate School

Pukyong National University

Abstract

The thickness dependent magnetic properties of artificially prepared ultrathin body-centered cubic Ni films have been explored using the all electron full potential linearized augmented plane wave (FLAPW) method. Here, we have considered two types of BCC Ni(001) films : (i) pure BCC Ni(001) and (ii)Au capped BCC Ni(001) in the range from 1 monolayer (ML) to 5ML of Au capping coverage. The average magnetic moments of pure BCC Ni(001)is about 0.63 μ_B and a typical surface enhancement is found with magnetic moment of 0.78 μ_B. In the presence of Au capping layer, the magnetic moment if interface Ni is strongly suppressed to approximately 0.5 μ_B and this cause the reduction of average magnetic moment. Nevertheless, the Au adlayer has no meaningful induced magnetic moment.

The BCC pure Ni(001) films have always in-plane magnetization up to 11 ML, but very interestingly the Au/Ni(001) shows thickness dependent spin reorientation transition(SRT) from in-plane to perpendicular to the film surface according to the Au coverage. However, the thickness dependent SRT shows very irregular behaviors.

In addition, the calculated X-ray absorption spectroscopy(XAS) and X-ray magnetic circular dichroism (XMCD) have been presented.

Chapter 1. Introduction.

In thin film magnetism, the materials composed of typical 3d transitional metal elements have been extensively explored. As well known, the Fe, Co, and Ni have body-centered-cubic(BCC), hexagonal-closed-packed(HPC), and face-centered cubic (FCC) crystal structures in bulk mode, respectively.

To date, the fundamental magnetic properties of these materials in bulk state are well understood. in the other hand due to the advanced atomic manipulation technique, it is possible to materialize artificial nano structure which does not exist in nature. For instance, Fe and Co used to have BCC and HPC crystal structure can maintain FCC phase under certain conditions. [15-17] This means that the thermodynamically stable crystal structure can be even tuned in an artificial way and it may bring a new opportunity to utilize the noble magnetic properties for potential magnetic device applications.

However, there was no report on the BCC type Ni and it has long been remained an intriguing issue to materialize BCC Ni for experimentalists until recently although the magnetic properties of BCC Ni have been studied using first principles method.[18-19] One may argue that many studies for the BCC Ni

on Fe(001) have been presented[25-28], but in this case it is obvious that the magnetism of BCC Ni affected by the hybridization with magnetic Fe surface.

In order to understand the intrinsic magnetism of BCC Ni, not affected by magnetic materials, one needs to grow BCC Ni on non-magnetic surface. Interestingly, it has been demonstrated that the bulk like BCC Ni on non-magnetic surface. Interestingly, it has been demonstrated that the bulk like BCC Ni can be epitaxially grown on GaAs(001) surface with a lattice constant of a=0.282nm [29-30]. According to the report by Tian et al.[29], the Ni/GaAs(001) manifests magnetic moment of about 0.53 μ_B and the bulk like BCC Ni has an in-plane cubic magnetocrystalline anisotropy energy of $4.7\times10^{5} ergs\,cm^{-3}$.

On theory side, several first principles calculations have been performed to reveal the magnetic properties of BCC Ni [31-33]. These theoretical studies show that the lattice distortion of BCC Ni does not substantially influence on the magnetic moment[31] and the calculated magnetic moment is not significantly deviated from the experimentally found value. Besides, a theoretical study for magnetic anisotropy of bulk like BCC Ni is presented.[32]

So, Thickness dependent magnetic properties of BCC Ni and Au capped on BCC Ni are calculated in this article using the

FLAPW (GGA) method.

"Full-potential linearized augmented plan wave" FLAPW has been known as exact method among first principles calculation methods until now. Especially, in 3d transition metal case, GGA method gives better results than Local density approximation (LDA) method, so Ni(BCC) have been calculated by the GGA approximation.

Chapter 2. Methodologies

2.1. Density Functional Theory (DFT)

A reduction of the complicated many-body problem to an effective single-particle theory which is amenable to numerical calculations and supplies deeper physical insight is the density functional theory due to by **Hohenberg and Kohn(1964)**[4], and **Kohn and Sham**(1965).[5]

Density functional theory is known as important tools for researching electron structure theoretically and provides very powerful ways to treat problem in many body system as a form of one particle system.

2.1.1. Hohenberg - Kohn theorem

Calculation for most first-principles is base on basic theory like density functional theory. Early DFT was found in Thomas-Fermi theory[1,2] which represented energy in ground state with only equation of density. Exact basis of DFT was formulated by Hohenberg - Kohn theorem[4].

This theorem supposes that the characteristic of ground state

in many body system could be presented with only density in ground state.

Therefore, exact calculation of density in ground state is proved to be possible from the principle included only density. Hamiltonian in many body systems could be written like as follow.

$$H = \hat{T} + \hat{V} + \hat{U} \tag{1}$$

Here $\hat{T}$, $\hat{V}$ and $\hat{U}$ represents Kinetic energy , external potential and Coulomb energy respectively. Given only external potential in the system we could find out total Hamiltonian. If system would be limited in non-degenerated systems corresponding eigenstate and density could be calculated with Schrodinger function

$$\hat{H}|\Psi = E|\Psi > \tag{2}$$

So function like $\hat{V} \rightarrow \Psi \rightarrow \rho(\vec{r})$ exists. Hohenberg - Kohn theorem supposes that function is one to one at ground state and invertible.

In other words external potential would be decided by electron density. This suggests various form of energy function

$$E_\nu[\rho] = <\Psi[\rho]|\hat{H}|\Psi[\rho]> = <\Psi[\rho]|\hat{T}+\hat{U}|\Psi[\rho]> + <\Psi[\rho]|\hat{V}|\Psi[\rho]> \quad (3)$$

$$E_\nu[\rho] = F_{HK}[\rho] + \int d\vec{r} v(\vec{r})\rho(\vec{r}) \quad (4)$$

and Hohenberg - Kohn function, $F_{HK}[\rho]$, would not be affected by external potential $\nu(\vec{r})$. Second equation of Hohenberg - Kohn theorem would be proved to be like

$$E_0 \leq E_v[\rho] \quad (5)$$

in any density ρ.

Here E_0 represents energy in ground state and would be stable only if $\rho=\rho_0$. ρ_0 represents density of ground state. So exact density of ground state could be decided with minimum of $E_\nu[\rho]$.

2.1.2. **Kohn-Sham Equation**

Hohenberg & Kohn, and **Kohn & Sham** have suggested that total energy in system like solid or surface is dependent on only charge density in ground state[4,5]

$$E = E[\rho] \tag{6}$$

The idea of using charge density in quantum mechanics theory to material had been started long time ago but only after decades that had been started to be adapted in molecule system with development of **Hartree-Fock** approximation and further in system of solid state. **Slater** used electron gas for calculation of solid state using **Hartree-Fock** approximation.

This method was X_α and has contributed for developing more sophisticated method of calculating electron structure.

Charge density is scalar function defined each point $\vec{r}$ in real space.

$$\rho = \rho(\vec{r}) \tag{7}$$

Charge density and total energy would be dependent on a kind and location of core atom like

$$E = E[\rho(\vec{r}), \overrightarrow{R_\alpha}] \tag{8}$$

In this $\overrightarrow{R_\alpha}$ is set of location of all atom α in any system considered. Eq.8 is an important one for understanding electron structure of material and dynamic characteristic in atom system and with this Eq.8 we could predict equilibrium of particles on the surface and cohesive energy of solid. And in this equation if total energy would be differentiate with the position of core of each atom we could get the force acting in that atom and find out stable structure of the system, therefore we could study dynamic procedure like diffusion or reaction of particles on the surface.

In DFT total energy Eq. 6 can be divided into kinetic energy, Coulomb energy and exchange-correlation like Eq. 9.

$$E = T_0 + U + E_{xc} \tag{9}$$

Coulomb energy U can be calculated with traditional method

and this can be divided into attraction between electron and core, repulsive force between electron and repulsive force between cores again.

$$U = U_{en} + U_{ee} + U_{nn} \tag{10}$$

U_{en}, U_{ee},and U_{nn} are represented Eq. 11~13

$$U_{en} = -e^2 \sum_{\alpha} Z_{\alpha} \int \frac{\rho(\vec{r})}{|\vec{r} - \vec{R}|} d\vec{r} \tag{12}$$

$$U_{ee} = e^2 \iint \frac{\rho(\vec{r})\rho(\vec{r}')}{|\vec{r} - \vec{r}'|} d\vec{r} d\vec{r}' \tag{13}$$

$$U_{nn} = e^2 \sum_{\alpha\alpha'}^{\alpha} \frac{Z_{\alpha} Z_{\alpha'}}{|\vec{R_{\alpha}} - \vec{R_{\alpha'}}|} \tag{14}$$

Kinetic energy T_o is more complicate. According to DFT actual electron in the system could be changed into effective electron with contribution of same charge, mass and density. Real electron is affected by all other electron but effective electron moves as particles not related to effective potential, so T_o can be represented with the sum of kinetic energy of all

effective electron.

If respectively effective electron would be stated with wave function Ψ_i of single particle, kinetic energy of all effective electron in the system could be represented with

$$T_o = \sum_i n_i \int \psi_i^*(\vec{r}) \left[\frac{-\eta^2}{2m} \nabla^2 \right] \psi_i(\vec{r}) d\vec{r} \qquad (14)$$

Eq. 14 is the sum of expected value to kinetic energy of a particle and n_i is defined as the number of electron in the state of i.

E_{xc}(exchange-correlation energy), last term of Eq. 9 is included energy by contribution of all extra complicate electron.

In this the most important contribution is the term of exchange term. An electron is fermion, so according to Pauli's exclusion principle, average coulomb repulsion act on electrons has been decreased due to an electron with the same spin is not impossible to exist on the same orbit that energy is called "exchange energy". If each electron would be considered to be surrounded with positive exchange hole, total electric charge

summed by all exchange hole could be +e . According to definition additional many body problem among electrons with opposite spin would be called as "correlation energy". Kinetic energy and Coulomb energy have opposite sign and almost same amount but exchange correlation energy is about 10% of Coulomb energy. Correlation energy is much smaller than exchange energy but plays an important role in conclusion of length and strength of atomic combination.

Binding energy of atoms on surface or solid is much smaller than total energy, so it ranges in about 1~8 eV and energy which would change position of atoms on the surface is also very small.

Most important Hohenberg-Kohn-Sham theorem in DFT represents that total energy under density of ground state would have minimum value like Eq. 15.

$$\frac{\partial \vec{E}[\rho]}{\partial \rho}|_{\rho=\rho_o} = 0 \qquad (15)$$

If wave function of single particle would be $\psi_i(\vec{r})$, electron

density, $\rho(\vec{r})$ could be stated as Eq. 16.

$$\psi_i(\vec{r}) = \sum_i n_i |\psi(\vec{r})|^2 \tag{16}$$

As Eq. 14 for kinetic energy n_i is defined as the occupation number in the eigenstate in which that would be represented with wave function of single particle, $\psi_i(\vec{r})$.

In Eq. 14~16 wave function of single particle has been used and variation in this wave function corresponds with variation of electron density, so the condition of single particle wave function under ground state density can be induced from the condition of calculus of variation of Eq.15. This formula is called as "**Kohn-Sham equation**"

$$\left[\frac{\vec{\eta^2}}{2m} \nabla^2 + V_{eff}(\vec{r}) \right] \psi_i(\vec{r}) = \epsilon_i \psi_i(\vec{r}) \tag{17}$$

In this $V_{eff}(\vec{r})$ is represented with Eq. 18.

$$V_{eff}(\vec{r}) = V_c(\vec{r}) + \mu_{xc}[\rho(\vec{r})] \tag{18}$$

The electron density which corresponds to this wave function would be density in ground state which would make total energy minimum. The solution of **Kohn-Sham** equation forms orthonormalized set of Eq. 19.

$$\int \psi_i^*(\vec{r})\psi_j(\vec{r})d\vec{r} = \delta_{ij} \tag{19}$$

Because in Eq. 9 total energy is divided into 3 terms Kohn-Sham equation has also 3 terms. Kinetic energy is second order differential operator of Shrodinger equation of single particle and is not related to the system. In contrast $V_c(\vec{r})$, operator of Coulomb potential, and μ_{xc}, operator of exchange correlation potential, are dependent on contribution of electron in considered system. $V_c(\vec{r})$, Coulomb potential, on point $\vec{r}$ are generated from charge of core and electron in the system and calculated immediately in real space like Eq. 20.

$$V_c(\vec{r}) = -e^2\sum_{\alpha}\frac{Z_\alpha}{|\vec{r}-\vec{R_\alpha}|} + e^2\int\frac{\rho\vec{r'}}{|\vec{r}-\vec{r'}|}d\vec{r'} \tag{20}$$

In condensed system for calculating Coulomb potential we should solve Poisson equation of Eq. 21.

$$\nabla^2 V_c(\vec{r}) = -4\pi e^2 q(\vec{r}) \tag{21}$$

Exchange correlation potential is related to exchange correlation energy like Eq 22.

$$\mu_{xc} = \frac{\partial E_{xc}[\rho]}{\partial \rho} \tag{22}$$

In actual calculation exchange correlation energy (or exchange correlation potential) is not well known and it could be calculated with approximation method like LDA or GGA etc.

2.1.3. Local density approximation (LDA)

All complicate phenomena of physics in interaction system could be solved by calculating standardized equation about $E_{xc}[\rho]$. It is natural to use characteristics of uniform electron gas interaction about density of slow variation. In other words put exchange correlation energy density is ϵ_{xc} it would be dependent on only $\rho(\vec{r})$, local density.

$$E_{xc}[\rho] = \int \rho(\vec{r})\epsilon_{xc}[\rho(\vec{r})]d\vec{r} \tag{23}$$

Exchange correlation energy is dependent on only local density of electron around of each $d\vec{r}$, volume element. This method of approximation is called as LDA.

LDA has two assumption, first the effect of exchange correlation would be domain only around the point and second the effect of that would not be dependent on variation of electron density around. Therefore in volume element it could be treated as the same density of electron.

So, It is same charge density at volume element. This approximation is very corrected in the system of metal but should be used with precaution in the system in which variation of electron density would be great.

We have make an effort to understand a system of electron with uniform density and research characteristics. Especially exchange correlation energy per electron of uniform electron gas has been calculated with various method of approximation like many body perturbation theory and Monte Carlo method. In actual calculation it would be represented analytic function of electron density and in expression of term of exchange correlation there are various analytic forms with different coefficient. For example in the system in which spin polarization would not be accounted for, the term of local density exchange by Kohn & Sham would be

$$\epsilon_x = -\frac{3}{2}\left(\frac{3}{\pi}\rho\right)^{\frac{1}{3}}, \qquad \mu_x = -2\left(\frac{3}{\pi}\rho\right)^{\frac{1}{3}} \tag{24}$$

and the correlation term by Hedin and Lundqvist would be

$$\epsilon_c(\rho) = -C\frac{e^2}{a_0}\left[(1+x^3)\ln(1+\frac{1}{x})+\frac{x}{3}-x^2-\frac{1}{3}\right] \quad (25)$$

Here, $C=0.0225$, a_0 is Bohr radius and

$$x = \frac{r_s}{21a_0} \quad (26)$$

$$r_s = \left[\frac{3}{4\pi\rho}\right]^{\frac{1}{3}} \quad (27)$$

Exchange correlation energy ϵ_{xc} and exchange correlation potential, μ_{xc} would be

$$\epsilon_c(\rho) = \epsilon_x + \epsilon_c \ , \ \mu_{xc} = \frac{\partial\rho\epsilon_{xc}}{\partial} \quad (28)$$

2.1.4. General Gradient Approximation (GGA)

LDA would not fit in the system in which electric charge would be localized like transition metal because in this method localized uniform electric charge of electron gas would be used in not uniform system. In LDA combination energy of particles and solid has been overestimate and gap of semi-conductor has been underestimate. And in calculation total energy of iron it is suggested that ferromagnetism of BCC would have lower energy. For complement of problems of LDA General Gradient Approximation has been recently developed[9,10].

General Gradient Approximation could derive much better result than L(S)DA in not uniform system because If consider gradient of electron density in each point in the space and gradient of electron density as well in the case of treating exchange correlation function. So, General Gradient

Approximation can be called "non local" potential also. GGA has been complemented by Perdew and Wang and up to now has been complemented continuously[10].

For example

$$E_{GGA} = E_{LDA} + E_x^G + E_c^G \tag{53}$$

and exchange E_x^G term suggested by Becke is

$$E_x^G = b\sum\int \frac{\rho_\sigma x_\sigma^2}{1+6bx_\sigma \sinh^{-1} x_\sigma} d\vec{r} \tag{54}$$

$$x_\rho = \frac{|\nabla\rho|}{\rho_\sigma^{\frac{4}{3}}} \quad , \quad \sigma = \uparrow \text{or} \downarrow \tag{55}$$

and E_c^G term suggested by Perdew is

$$E_c^G = \int f(\rho_\uparrow, \rho_\downarrow) e^{g(\rho)|\nabla\rho|} |\nabla\rho|^2 d\vec{r} \tag{56}$$

2.1.5. Method of Full potential Linearized Augmented Plane Wave (FLAPW)

The most important fact which should be accounted for in calculating electro structure of material is interaction in the many body system of electrons. Because complicate interaction among electrons would decide various and subtle property of material. But generally LDA by DFT will be used because actually interaction among countless electrons over Avogadro's number would be impossible to be treated directly.

DFT established by Hohenberg and Kohn is based on the theorem in which energy has minimum value when energy in ground state in the many body system would be important DFT of electric charge density and charge density of ground state.

And with LDA a potential on a point could be represented with density of electric charge on that point, so kinetic equation of quantum mechanics in the many body system could be represented with equation of single particle like Kohn-Sham equation. Accordingly if you would like to research electron

structure you would solve Kohn-Sham equation numerically. For equation solution of single particle by DFT there are various ways according to method of statement of wave function, electric potential, exchange correlation potential and relativistic consideration of Kohn-Sham equation.

Method of FLAPW is known for the most precise calculation method of Kohn-Sham equation up to now and it has been widely used for research of various materials. And for calculating property of surface and interface single slab structure would be used. Single slab divides into 3 area in real space that is Muffin tin around core, vacuum both ends of thin slab and interstitial and would be calculated in consideration of each area. In this moment wave function in each area shall be developed as basis function according to geometric forms.

That is, sphere spherical harmonics put the basis function in MT and 2-dimensional linear function in vacuum area and 3-dimensional plane wave function in interstitial area . Wave function in each area would be linear, in other words wave function should be composed in consideration of first order

differentiation function and be continuous on the boundary in each area. Static potential in equation of single particle would be decided by solving Poisson equation with method of pseudocharge designed by Weninert[11]. Exchange correlation potential would be calculated by Least Square Method with use of function form of Hedin-Lundqvist[6]or Von Varth-Hedin[7] in which density of charge would have been given like . The important electron system is treated relativistically and valence electron is treated in proportional relativistically in consideration with all relativistic terms except for the term of interaction of spin-orbit. Method of FLAPW could also derive much more precise result because the approximation according to form like electron spin density and potential etc would never been used. Likewise Method of FLAPW could be stated as the method for exact calculation of various magnetism on the surface and interface and rearrangement on the surface as well in comparison with other methods[12].

If wave function of single particle $\psi(\vec{k},\vec{r})$ would be developed to reciprocal lattice G the result would be as follow

$$\psi(\vec{k},\vec{r})\sum_{G} c_{i,k}(G)\phi(\vec{k}+\vec{G},\vec{r}) \tag{57}$$

Here each basis function ϕ is Linear Augmented Plane Wave: LAPW given in following formula.

$$\phi(\vec{k}+\vec{G},\vec{r}) = \Omega^{-1/2} e^{i(k+G)r}$$

$$\vec{r} \in \bigcap stitial$$

$$\phi(\vec{K}+\vec{G},\vec{r}) = \sum_{L}[\overrightarrow{A_L}(\vec{K}+\vec{G})\overrightarrow{U_l}(\vec{E_l},\vec{r}) + \overrightarrow{B_l}(\vec{K}+\vec{G})\dot{u}(\vec{E_l},\vec{r})]\overrightarrow{Y_l}(\hat{r})$$

$$\vec{r} \in MTsphere$$

$$\phi(\vec{K}+\vec{G},\vec{r}) = \sum_{v}[\overrightarrow{A_v}(\vec{K}+\vec{G})\overrightarrow{u_{\vec{K}+\vec{G}}}(\vec{E},z) + \overrightarrow{B_v}(\vec{K}+\vec{G})\dot{u}_{\vec{K}+\vec{G}}(\vec{E_v},z)]\overrightarrow{e^{j(\vec{K}+\vec{G})r}}$$

$$\vec{r} \in vacuum$$

(58)

Element of G is defined from the thickness of thin slab and Ω is the volume of unit cell. Radial function $u_l(E_l,\vec{r})$ is energy E_l regulated in muffin-tin sphere and would be solved with solution of radial Schrodinger equation with spherical

effective potential.

$$\frac{1}{\vec{r}}\frac{d^2}{d\vec{r}}(\vec{r}u_l)-\frac{l(l+1)}{\vec{r}^2}u_l+2(\vec{E_l}-\vec{V})u_l=0 \qquad (59)$$

$\dot{u}(E_l,\vec{r})$ is a differentiation of energy of u_l and it satisfies form of differentiation of that, so it would be

$$\frac{1}{\vec{r}}\frac{d^2}{d\vec{r}}(\vec{r}\dot{u})-\frac{l(l+1)}{\vec{r}^2}\dot{u}+2(E_l-V)\dot{u}+2u_l=0 \qquad (60)$$

And u_l is standardization and, u_l **and** $\dot{u_l}$ **is orthogonal, so** it would be stated as follow

$$\int_0^{R_{MT}}\vec{r}^2u_l\dot{u}d\vec{r}=0 \qquad (61)$$

Coefficient A_L and B_L is decided satisfying spherical boundary condition of basis function ϕ and its differentiation $\frac{\partial\phi}{\partial\vec{r}}$. Similarly Z dependency function $u_{k+G}(E_\nu,z)$ and differentiation of energy $\dot{u_{k+G}}(E_\nu,z)$ are derived by solution of

one dimension Schrodinger equation like following formula.

$$[\frac{\partial^2}{\partial z^2}+2(E_v-V(z)-(\vec{K}+\overrightarrow{G^2})]u_{K+G}=0 \tag{62}$$

$$[\frac{\partial^2}{\partial z^2}+2(E_v-V(z)-(\vec{K}+\overrightarrow{G^2})]\dot{u}_{K+G}=0 \tag{63}$$

Continuous condition of ϕ and $\frac{\partial\phi}{\partial\vec{r}}$ on the boundary of vacuum will be used for deciding A_v and B_v.

In Method of FLAPW $n(r)$, charge density would be stated with 3 area as follow.

$$\begin{aligned} n(\vec{r}) &= \sum_G n_G\, e^{iG\cdot r} \quad r\in\bigcap stitial \\ n(\vec{r}) &= \sum_L n_L(\vec{r})\; Y_L(\hat{r}) \quad r\in MTsphere \\ n(\vec{r}) &= \sum_G n_G(z)\; e^{iG\cdot r} \quad r\in vacuum \end{aligned} \tag{64}$$

Coulomb potential could be derived with solution of Poisson equation and effective single particle potential which has been given in sum of Coulomb potential and correlation exchange potential would be represented with the form of density of

charge given in formula 64. Finally secular equation would be as follow.

$$\sum_{G} [H_{G,G'} - \epsilon_i (\overrightarrow{k}) O'_{G,G}] c_{i,k} (\overrightarrow{G}) = 0 \qquad (65)$$

Here, $H_{G,G'}$ is Hamiltonian matrix in K-S equation and $O_{G,G'}$ is overlap matrix. As concept of linearization with Method of LAPW radial function could be developed from random E to term of $u_l(E_l)$ and $\dot{u_l}(E_l)$.

$$u_l(E) = u_l(E_l) + \delta \dot{u}(E_l) \qquad (66)$$

Here, δ would be decided by coefficient of A_L and B_L in Eq.58 satisfying a boundary condition of Muffin-tin sphere.

2.2. Methodology for determining MCA

The Magneto-Crystalline Anisotropy energy(MCA) is defined as the difference of the total energy for two different magnetization orientations, that is, in-plane and perpendicular. The direct approach, where the MCA is calculated by comparing the total energies between the two magnetic orientations, has a technical difficulty concerning the numerical stability of calculating a very small difference of two large numbers; the total energy is estimated to 30,000~40,000eV/atom for bulk Fe, Co and Ni, for example, while MCA is the order of $10^{-4}eV$(thin films) - $10^{-6}eV$ (bulk). In fact, in order to calculate the total energy with this accuracy so as to eliminate numerical fluctuations, extremely fine sampling meshes are required for the k-space integrations.

Fortunately this difficulty is solved by applying the force theorem.[34] Starting with the variational expression for the total energy in density functional theory as given in Eq. 67,

$$E_{tot} = \sum_{i}^{occ} \epsilon_i - \frac{1}{2} \iint d\vec{r}\, d\vec{r}' \frac{n(\vec{r})n(\vec{r}')}{|\vec{r}-\vec{r}'|} + \int d\vec{r} n(\vec{r}) \left[\epsilon_{xc}(n(\vec{r})) - \mu_{xc}(n(\vec{r})) \right]. \tag{67}$$

the force theorem has proven that :

1. Given an exact density, ρ_0, the total energy estimated from the trial density ρ is correct to the second order of the charge variation, i.e.

$$E[\rho] = E[\rho_0] + O[(\rho - \rho_0)^2] \tag{68}$$

2. If there are two crystal structures, α and β with charge density ρ_α and ρ_β, the difference in total energy estimated from the same charge density, $E_\alpha[\rho_\alpha] - E_\beta[\rho_\alpha]$, can be approximated as the difference in the sum of the single-particle eigenvalues due to systematic cancellations of other terms.

This force theorem can be applied to MCA calculations. In the second variational treatment of spin orbit coupling (SOC), we start with the scalar relativistic self-consistent charge/spin density $\rho_0(\vec{r})$ and $\overrightarrow{m_0}(\vec{r})$, and the corresponding scalar relativistic total energy, $E_0[\rho_0, \overrightarrow{m_0}]$ which is given as Eq. 67. If we assume that the scalar relativistic plus SOC calculations yield the charge/spin density $\rho(\vec{r})$ and $\overrightarrow{m}(\vec{r})$ and the corresponding total energy $E[\rho, \overrightarrow{m}]$, the SOC induced energy

can be written as

$$E_{sl} = E[\rho, \overrightarrow{m}] - E_0[\rho_0, \overrightarrow{m_0}]$$

$$= (E[\rho, \overrightarrow{m}] - E[\rho_0, \overrightarrow{m_0}]) + (E[\rho_0, \overrightarrow{m_0}] - E_0[\rho_0, \overrightarrow{m_0}]) \quad (68)$$

According to the force theorem point 1, we see that the first bracketed term in Eq. 68 is negligible to first order of the charge/spin density variations induced by the SOC. On the other hand, the second point of the force theorem ensures that the second term of Eq. 68 , which is the difference in total energy with and without SOC estimated from the scalar relativistic charge/spin densities, can be approximated as the difference in two sums of single-particle energies with and without SOC, as

$$E[\rho_0, \overrightarrow{m_0}] - E_0[\rho_0, \overrightarrow{m_0}] \simeq \sum_{i,\vec{k}}^{occ} \epsilon_i(\hat{m}, \vec{k}) - \sum_{i,\vec{k}}^{occ} \epsilon_i^0(\vec{k}) \quad (69)$$

The validity of this approximation was proven explicitly for surfaces/interfaces by estimating that the variation of the charge density induced by SOC if of second order in the SOC strength, namely, $\delta_\rho \sim \xi^2$ and thus the correction to the MCA force theorem is order of ξ^4 , while the typical surface/interface

MCA is order of ξ^2[35].

From the force theorem, the MCA ΔE_{sl}, defined as the difference of the total energy for in-plane($\theta=90^o$) and perpendicular($\theta=0^o$) magnetization orientations, can be written as

$$\Delta E_{sl} \equiv E(\hat{m}_{\theta=0^o}) - E(\hat{m}_{\theta=90^o}) = \sum_{i,k}^{occ(90)} \varepsilon_i(\overrightarrow{m}(\theta=90^o),\vec{k}) - \sum_{i,k}^{occ(90)} \varepsilon_i(\overrightarrow{m}(\theta=0^o),\vec{k}) \quad (70)$$

This seems feasible to calculate MCA from the sums of Kohn-Sham eigenvalues rather than from the total energies since the former is order of 10eV for the 3d transition monatomic systems. However, the result calculated with this method still reported a large fluctuation and thus slow convergence of the calculated MCA with respect to the number of k-points.[36,37]

The rotation of the magnetization from 0^o to 90^o leads to a redistribution of the occupied states. The the occupied sets $\{occ(90^o)\}$ and $\{occ(0^o)\}$ in Eq. 70 are independently determined according to Fermi statistics by their own eigenvalues, $\epsilon_i(\hat{m}(90^o))$ and $\epsilon_i(\hat{m}(0^o))$, respectively, to ensure particle

conservation.

Wang et al[38] pointed out a possible error introduced in this procedure, which might violate the validity of the force theorem due to large charge/spin density variations. As a reasonable way to obtain the new occupied states of the SOC Hamiltonian, they proposed a so-called state tracking method. In the state tracking method , each of the new occupied states $\{occ(90^o)\}$and $\{occ(0^o)\}$(with SOC) are determined by maximizing the probability of the new occupied sets to be found in the old occupied states (without SOC), which allows the perturbed state to obtain spatial distributions of the charge and spin densities as close as possible to the unperturbed states. This method is reported to efficiently depress the severe fluctuation of the MCA with respect to the number of k points [38-40]

More recently , the torque method[41] was proposed as another way to simplify the MCA calculation by realizing that the definition of MCA is equivalent to the partial derivative of SOC energy with respect to θ calculated at $\theta=45^o$. For example, for the surface with 4-fold rotational symmetry, where the φ dependence of the MCA is negligible, and the SOC energy has the form $E_{sl}(\theta) = K^{(2)}\sin^2(\theta) + K^{(4)}\sin^4(\theta)$, then

$$T(\theta = 45^o) \equiv \frac{E_{sl}(45^o)}{d\theta} = - K^{(2)} - K^{(4)}$$

$$= E_{sl}(\theta = 90^o) - E_{sl}(\theta = 0^o) \equiv \triangle E_{sl.} \qquad (71)$$

In practice, the torque is calculated by applying the Hellman-Feynman theorem as

$$T(\theta) = \sum_{i,k}^{occ} < \psi_{i,\vec{k}} | \frac{\partial H_{sl}}{\partial \theta} | \psi_{i,\vec{k}} > . \qquad (72)$$

Where $\psi_{i,\vec{k}}$ is the wave function of the SOC Hamiltonian, H_{sl}. The advantage of the torque method is that there is only one Fermi energy to be estimated which suppresses the fluctuations due to the independently determined Fermi energies of the perturbed and the unperturbed states as mentioned above. The state tracking method still can be used to determine the new occupied states for the SOC Hamiltonian, an advantage that may not be critical. However, there is a trade-off in using the torque method; the magnetization oriented along $\theta = 45^o$ reduces the symmetry for most systems, which results in a larger IBZ and thus an increased number of k-points.

Recently, the self-consistent second variational method was also employed to achieve better convergence of MCA calculation[42] where instead of the scalar relativistic solution, the charge density with SOC for perpendicular magnetization was obtained self-consistently in a second variational way and used to estimate the MCA for the in-plane magnetization by applying the force theorem. However, it didn't reveal any significant improvement over the non-self-consistent approach for 3d transition metals.

In our calculations , we used the non-self-consistent second variational approach for SOC inclusion. The MCA was obtained by the torque method with the new occupied states (with SOC of $\theta = 45^{o}$) determined by the state tracking method.

Chapter 3. Numerical Method.

The thin film version of full potential linearized augmented plane (FLAPW) method is employed in our calculations. Therefore, no shape approximation is assumed in charge, potential, and wavefunction expansions[20-22]. We treat the core electrons fully relativistically, and the spin orbit interaction among valence electrons are dealt with second variationally[23]. The generalized gradient approximation is used to describe exchange correlation[24]. Spherical harmonics with l_{max}=8 are used to expand the charge, potential, and wavefunctions in the muffin tin region.

Energy cut offs of 225 Ry and 13.7 Ry are implemented for the plane wavefunction and basis expansions in the interstitial region.

We use 210 k-mesh points during the course of entire calculations discussed in this report. Since it is found that the BCC Ni grown on GaAs(001) has a lattice constant of 0.282nm, we employ the same lattice parameters in lateral direction. To investigated the effect of Au capping on the thickness dependent magnetic anisotropy of Ni film, we assume that the Au adlayer can also be grown on BCC Ni

pseudomorphically, while the vertical positions of all constituents are optimized via force and total energy minimization procedures. Here, we have considered in the range from 5ML to 11ML Ni thickness and the thickness of Au capping layer is increased up to 4ML coverage.

Chapter 4. Result

4.1. Structural Feature

We have calculated the optimized atomic position and vertical distance using the total energy and force minimization procedure. We first show the optimized atomic structures and pure BCC Ni and Au capped systems in Table 4.1.1 and Table 4.1.2. Table 4.1.1 use the GGA approximation and Table 4.1.2 use the LDA approximation. And Figure 4.1 is Schematic side view of the Au/Ni ultra-thin film structure. In Figure 4.1, the Ni at the interface between Ni and Au adlayer is represented by Ni_s and the subsurface layer is denoted by Ni_{s-1}. The Au_i stands for i-th adlayer counted from the interface. Also, $d(Ni_{s-i}\text{-}Ni_{s-i})$ means calculated vertical distance between two neighbor atoms as in Fig 4.1 and the values are given in Table 4.1.1 and Table 4.1.2.

Note that we have only displayed the optimized vertical distances with 11ML of Ni thickness in Au/Ni system. In other Au/Ni systems, there was found no physically meaningful change . As mentioned earlier, the bulk like BCC Ni has a

lattice constant of 0.282 nm and one can see that the calculated vertical distances of pure Ni are close to this bulk value at the inner layer at the GGA approximation But the LDA approximation is not close to this bulk value. So, GGA approximation has the correct value in Ni(BCC).

You can see that the inward relaxation is found at the surface layer. In the Au/Ni(11ML), the interlayer distances of Ni are suppressed by less than 0.1 Å near the interface region, whereas the distances of inner layers are only slightly changed.

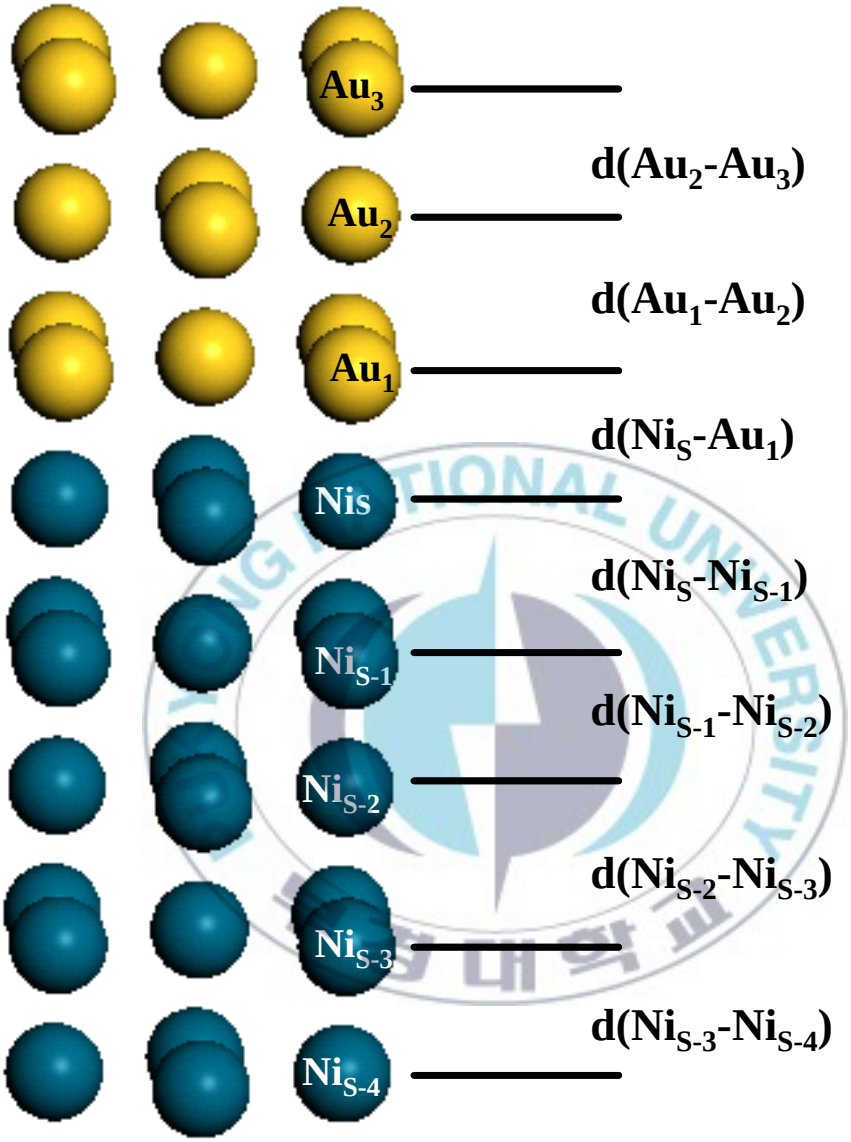

Fig 4..1. Schematic side view of the Au/Ni ultra thin structure.

thickness	Ni				Au			
	5ML	7ML	9ML	11ML	1ML	2ML	3ML	4ML
$d(Ni_{s-5}\text{-}Ni_{s-4})$				1.40	1.39	1.39	1.38	1.38
$d(Ni_{s-4}\text{-}Ni_{s-3})$			1.37	1.38	1.39	1.37	1.38	1.36
$d(Ni_{s-3}\text{-}Ni_{s-2})$		1.40	1.37	1.41	1.40	1.37	1.36	1.37
$d(Ni_{s-2}\text{-}Ni_{s-1})$	1.43	1.40	1.40	1.44	1.37	1.35	1.35	1.35
$d(Ni_{s-1}\text{-}Ni_{s})$	1.34	1.36	1.32	1.37	1.36	1.33	1.33	1.33
$d(Ni_{s}\text{-}Au_{1})$					1.76	1.75	1.75	1.75
$d(Ni_{s}\text{-}Au_{2})$						2.21	2.23	2.23
$d(Ni_{s}\text{-}Au_{3})$							2.22	2.23
$d(Ni_{s}\text{-}Au_{4})$								2.21

Table 4.1.1 Optimized interlayer distances(in Å) of pure BCC and Au/Ni films(GGA).

thickness	Ni				Au			
	5ML	7ML	9ML	11ML	1ML	2ML	3ML	4ML
$d(Ni_{s-5}\text{-}Ni_{s-4})$				1.25	1.25	1.25	1.25	1.26
$d(Ni_{s-4}\text{-}Ni_{s-3})$			1.25	1.25	1.25	1.25	1.26	1.24
$d(Ni_{s-3}\text{-}Ni_{s-2})$		1.27	1.26	1.27	1.26	1.26	1.26	1.26
$d(Ni_{s-2}\text{-}Ni_{s-1})$	1.32	1.27	1.26	1.25	1.27	1.27	1.27	1.27
$d(Ni_{s-1}\text{-}Ni_{s})$	1.20	1.20	1.25	1.21	1.27	1.26	1.26	1.26
$d(Ni_{s}\text{-}Au_{1})$					1.68	1.69	1.69	1.69
$d(Au_{1}\text{-}Au_{2})$						2.06	2.23	2.01
$d(Au_{2}\text{-}Au_{3})$							2.22	2.06
$d(Au_{3}\text{-}Au_{4})$								2.05

Table 4.1.2. Optimized interlayer distances(in Å) of pure BCC and Au/Ni films(LDA).

4.2. Magnetic Moment

In Table 4.2, we present the calculated magnetic moments. The average magnetic moment of pure Ni is in the range from $0.63\,\mu_B$ to $0.66\,\mu_B$ and this is somewhat large than that found in bulk like BCC Ni in which a magnetic moment of $0.53\,\mu_B$ is reported[29]. This enhanced average magnetic moment definitely stems from the well known surface enhancement as one can see from the calculated moment. In the presence of Au capping layer, the average magnetic moment is suppressed and it is in the range from $0.57\,\mu_B$ to $0.58\,\mu_B$. The magnetic moment of interface Ni_s adjacent to the Au adlayer is significantly affected and this contributes to the reduction of average magnetic moment.

It is observed that the magnetic moments of Ni is almost unchanged after 2ML Au capping. We have found the same trends in other systems although the Au/Ni (11ML) is only shown in Table 4.2.

thickness	Ni				Au			
	5ML	7ML	9ML	11ML	1ML	2ML	3ML	4ML
Ni_{s-5}				0.57	0.60	0.58	0.57	0.57
Ni_{s-4}			0.61	0.60	0.58	0.59	0.60	0.59
Ni_{s-3}		0.53	0.56	0.56	0.60	0.59	0.58	0.59
Ni_{s-2}	0.53	0.58	0.57	0.58	0.55	0.55	0.56	0.55
Ni_{s-1}	0.64	0.65	0.66	0.67	0.64	0.59	0.58	0.59
Ni_{s}	0.78	0.78	0.78	0.79	0.55	0.50	0.49	0.49

Table 4.2. Calculated magnetic moments (in μ_B)of pure Ni film and Au capped Ni films

4.3. Density of State

We now discuss the density of state (DOS) both of pure BCC Ni and Au/Ni films. In Figure 4.3. (a) and (b), the DOS of pure Ni and Au capped systems with 11ML Ni thickness are presented, respectively (the first few layers are shown).
One can see that the majority spin states are quite small at the Fermi level, while the minority states are sizable. Thus, the BCC Ni has close to half metallic feature. All the Ni layers manifest similar behaviors in both majority and minority spin states at the Fermi level.

From Figure 4.3. (a), it is found that the number if holes in majority spin bands are almost the same, whereas the Nis has more holes in minority spin bands compared with those in other atoms.This results in well known surface enhancement in Ni_s.

In Figure 4..3. (b), we display the DOS of Au(1ML)/Ni(11ML)film. As shown, the main features of DOS of Ni_s and this can nicely account for the trends in calculated magnetic moments in Table. 4.3.

In the Ni_s , it is seen that the minority spin states of Ni_s is shifted to the left compared with that in pure case and this

cause reduction in empty holes, while the majority spin holes are almost the same. Consequently, we can see suppressed surface magnetic moment in Ni_s.

For other layers, the change in minority spin holes are negligible. It is clear that this changes arises owing to the hybridization with Au atom as one can see from the DOS of Au adlayer in Fig.4.3. (b) (green line).

We have also explored the DOS features for other systems and have obtained very similar trends although they are not presented here.

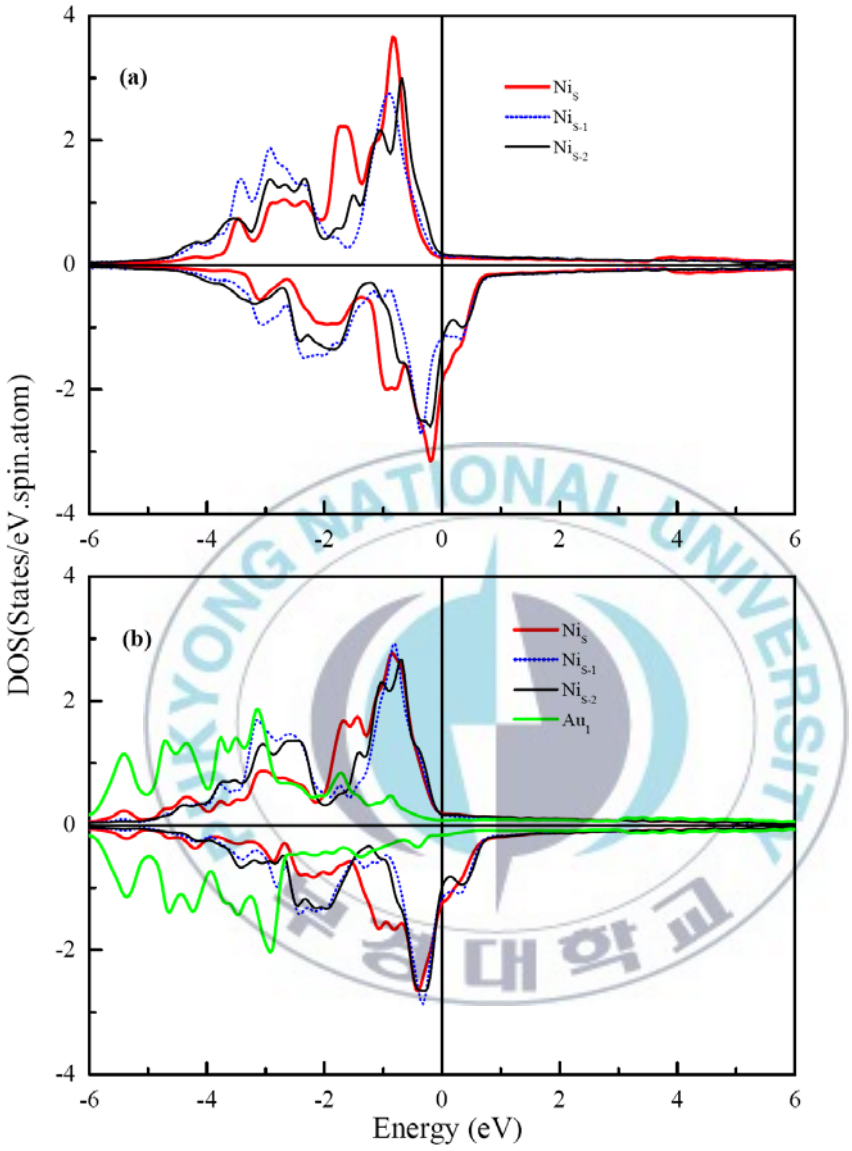

Figure 4.3. DOS of (a)pure BCC Ni (b)Au(1ML)/Ni(11ML). Here, the thickness of Ni is 11ML. DOS of Au/Ni

4.4. Magnetic anisotropy.

The main issue of this report is to investigate the thickness dependent magnetic anisotropy of ultrathin BCC Ni and Au/Ni films. The magnetic moment is simply a difference in the number of majority and minority spin electrons below the Fermi level and it has nothing to do with the wavefunction characters of occupied states.

However the magnetic anisotropy arising from a spin-orbit coupling depends on the wave function feature and this may indicate that the direction of magnetization is strongly affected by subtle changes in underlying electronic structure. Since the magnitude of the spin-orbit interaction is usually small, it is thus required to employ very accurate numerical methods to deal with the spin-orbit interaction resulting from relativistic effect.

To this aim, we use the torque method[43]. It has been known that the torque method provides very stable results even with fewer k-points compared to methods that employe different schemes since the torque method calculates the magnetic anisotropy energy via expectation values of the angular derivative of the spin-orbit Hamiltonian.

We will calculate both $E_1 = E_{100} - E_\perp$ and $E_2 = E_{110} - E_\perp$ where

E_{100} , E_{110} and $E_{\perp}$ stand for the total energy when the direction of magnetization points to the (100) and (110) direction with in-plane magnetization, while the $E_{\perp}$ means a total energy for perpendicular magnetization, respectively.

Through this, we can find a cubic magnetic anisotropy energy $K_1 = E_1 - E_2 = E_{100} - E_{110}$ for in-plane magnetization systems and an uniaxial perpendicular magnetic anisotropy energy $K_u = E_{100(110)} - E_{\perp}$. The negative K_1 stands for in-plane magnetization in (100) direction, while the positive K_1 means in-plane magnetization along the (100) direction. The calculated resulted results are shown in Table4.3.4. It is well known that the FCC Ni/Cu (100) film manifests SRT from in-plane to perpendicular to the film surface at the thickness of 7-10ML and the magnetic anisotropy can also be tuned due to oxygen effect [44].

Here, as shown above, there is no such a thickness dependent SRT from in-plane to perpendicular direction in ultrathin BCC Ni films at least until 11ML thickness. One can see that the 5ML Ni film has a magnetization along the (110) direction and all other BCC Ni films have an easy axis along the (100) direction.

Very interestingly, the Au capped ultrathin BCC Ni films

display quite different magnetic anisotropy from that of pure Ni film. For instance, the Au(1ML)/Ni(5ML) still shows in plane magnetization, but the magnitude of cubic anisotropy is greatly changed. In Au(2ML)/Ni(5ML), a large perpendicular anisotropy of Ku=158 μeV per Ni atom is realized. In Au/Ni(11ML), we also see SRT from in-plane, i.e. (100)direction, magnetization to perpendicular direction at 1ML Au coverage and then the direction of magnetization to perpendicular direction at 1ML Au coverage and then the direction of magnetization changes from perpendicular to the film surface to (110) direction (in-plane magnetization) by adding more Au layers.

The calculated results definitely show that the influence of interface contribution plays an essential role in determining the direction of magnetization, but the overall behaviors are not consistent with increasing Au capping. Therefore, the conventional interpretation in terms of competition among surface, interface, and volume part may not be applicable to this ultrathin film structure because it is not clear to separate each contribution. On theory side, the generalized relation between magnetic anisotropy and orbital anisotropy has been preposed by Van der Laan[45] but this correlations is not yet clear[46].

Au coverage	0	1ML	2ML	3ML	4ML
K_1					
Ni(5ML)	0.52	0.04			
Ni(7ML)	-0.11	4.8			0.8
Ni(9ML)	-0.18				
Ni(11ML)	-0.16		-2.73	3.82	2.06
K_U					
Ni(5ML)			151	150	89
Ni(7ML)			68	35	
Ni(9ML)		75	70	46	44
Ni(11ML)		19.7			

Table 4.4 : Calculated magnetic anistoropy energies per Ni atom (in μeV)

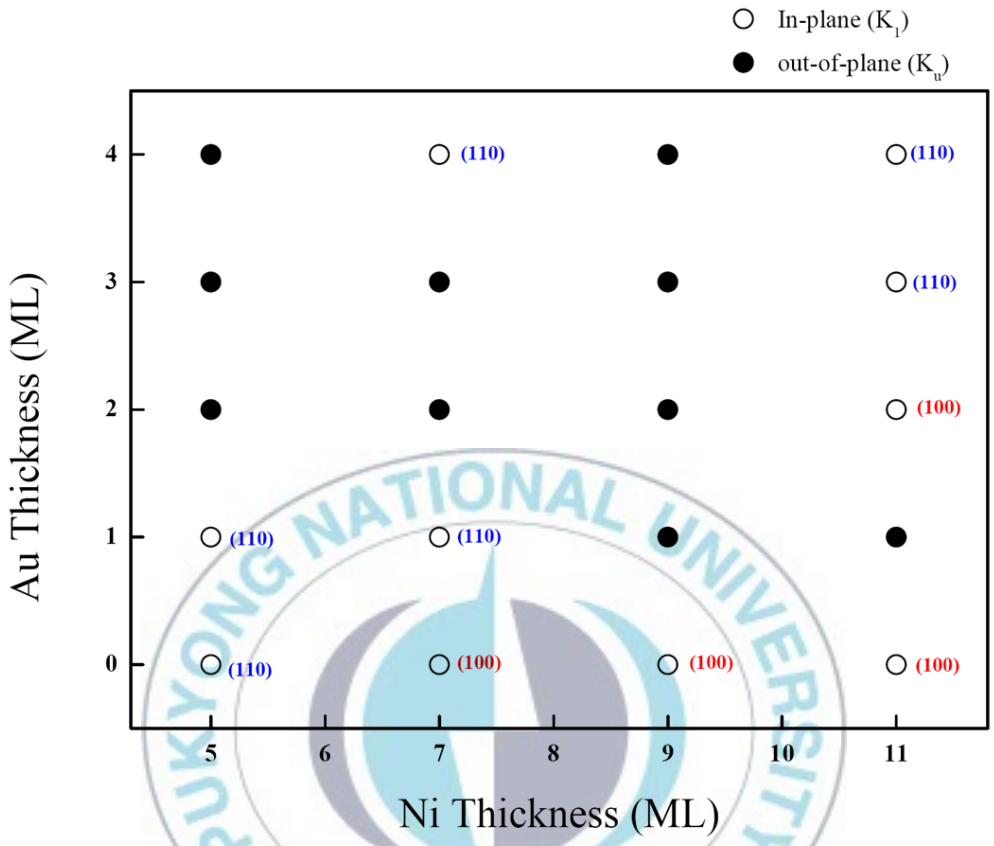

Figure 4.4.1 Calculated magnetic anistoropy energies

We therefore present the distribution of magnetic anisotropy over two dimensional Brillouin zone(BZ). The contribution to perpendicular magnetization at a given k-point is represented by red circle, while the blue circle is for contribution to in-plane magnetization. The magnitude of magnetic anisotropy is proportional to the size of circle. As a representative illustration for the MAE distribution, the distribution of 11ML pure Ni, Au(1ML)/Ni, Au(2ML)/Ni, and Au(3ML)/Ni are shown in Fig. 4.4.2, respectively. As shown in Fig. 4.4.2 (a) for 11ML of pure Ni film, the strong in-plane contributions to the magnetic anisotropy mainly arise from the 2D BZ boundary and around the circumference radius of $\pi/2a$.

In the presence of 1ML of Au capping as in Fig 4.4.2 (b), the in-plane contributions from the BZ boundary are significantly suppressed. On the other hands, one can see more contributions to the perpendicular magnetization approximately in the line of kx direction. As a result, a perpendicular magnetization to the film surface is achieved. Adding more Au layer, one can see different behaviors and this implies that the character of wavefunction is greatly modified. We also realize that there is no single dominant k-point contributing to the

magnetic anisotropy, so the Γ point analysis performed in bulk FeCo alloy[47] is not allowed.

Instead, it has been obtained that the many counteracting contributions are competing and the influence is accumulative.

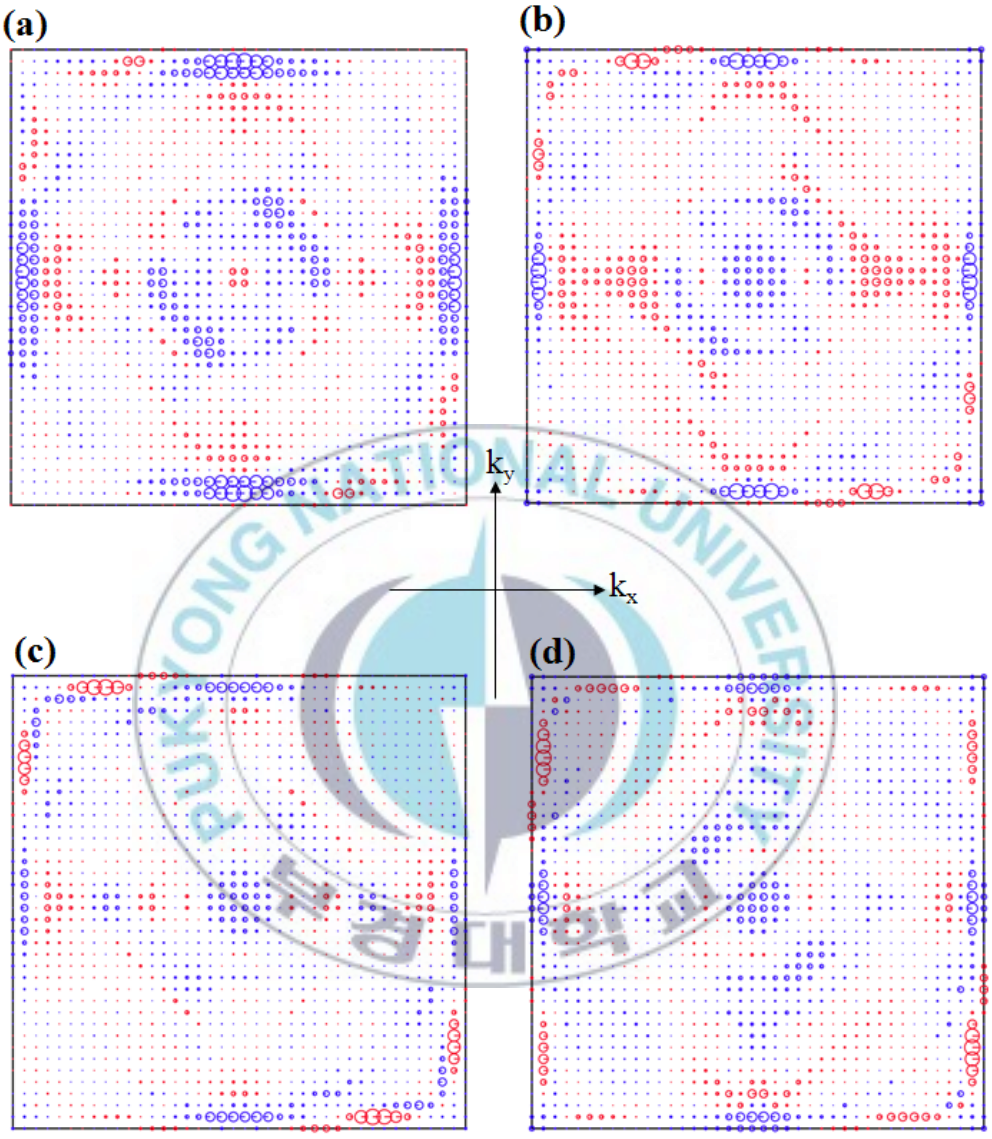

Figure4.4.2. Distribution of magnetic anisotropy over two-dimensional BZ (a)pure BCC Ni(11ML) (b)Au(1ML)/Ni(11ML), (c)Au(2ML)/Ni(11ML) (d)Au(3ML)/Ni(11ML).

4.5. X-ray absorption spectroscopy (XAS) and X-ray magnetic circular dichroism (XMCD) spectra.

In Fig 4.5, the calculated X-ray absorption spectroscopy (XAS) and X-ray magnetic circular dichroism (XMCD) are presented. Here, we only consider dipole transition assuming rigid core-hole reliazation. Thus, the exact peak position should be shifted if one compares the calculated results with experimental data. The Donish-Sunjic shape[48] with 0.12eV for life time broadening. We show the results of pure Ni and Au/Ni with 11ML film thickness.

The XAS and XMCD of pure Ni and Au capped systems are almost identical although the intensity of XMCD in Au/Ni is slightly suppressed. Due to rather simple unoccupied DOS above the Fermi level in Fig 1, we have well separated L edges XMCD. The peak position of Nis L edge is shifted to the left and this can be understood from the calculated DOS in Fig. 1.

The calculated orbital magnetic moment of Nis is 0.09 μ_B for pure Ni and it is reduced to 0.04 μ_B due to Au(1ML) capping . We have found about 0.04 μ_B at inner layers. Please note that the spectral shapes of XAS and XMCD for other systems are not presented here, but we have realized that there has been found no physically meaningful changes.

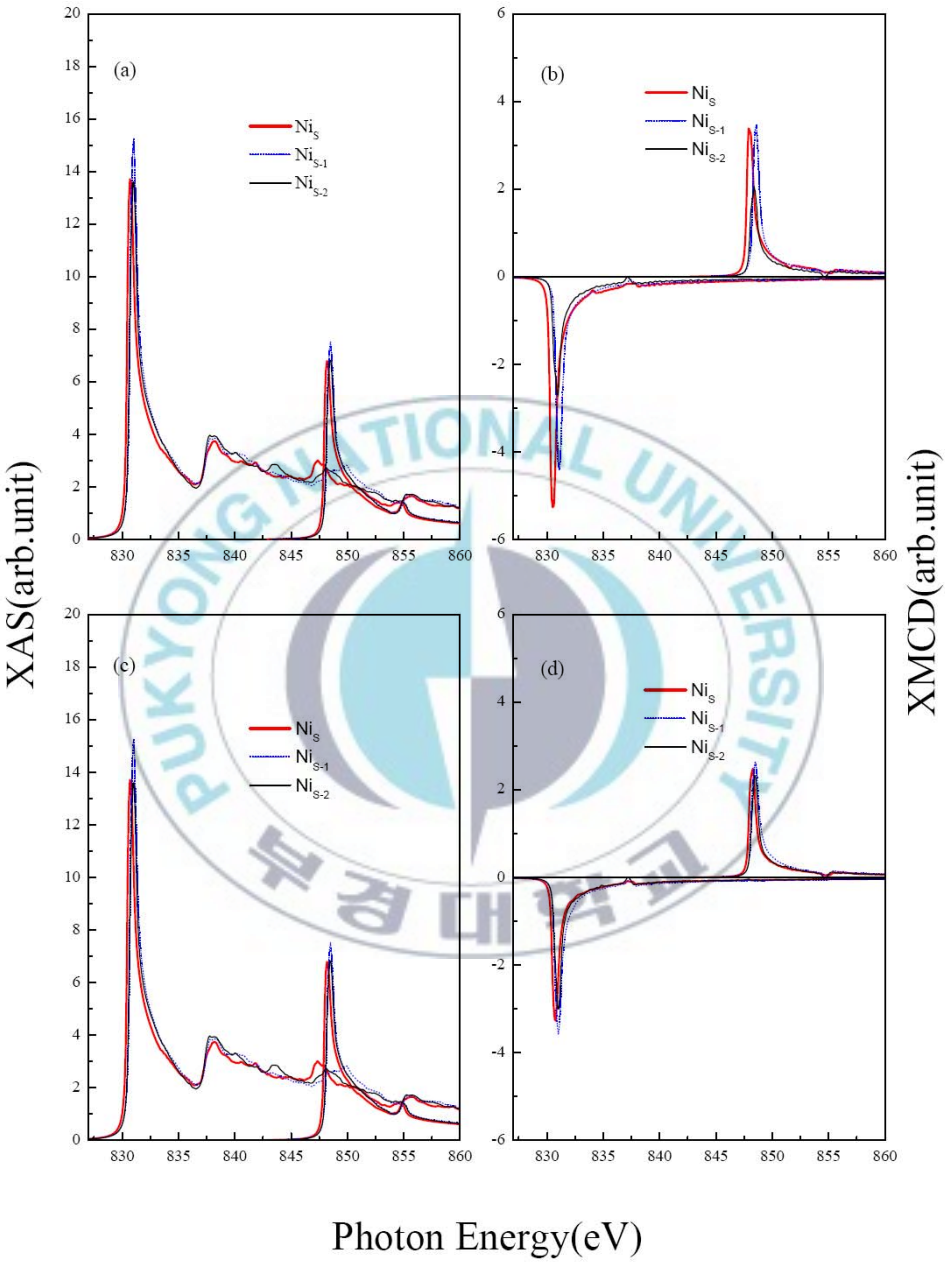

Fig 4.5 the calculated X-ray absorption spectroscopy (XAS) and X-ray magnetic circular dichroism (XMCD)

Chapter 5. Summary

In conclusion, we have investigated the thickness dependent magenetic anisotropy of ultrathin pure BCC Ni and Au/Ni systems.

Both BCC Ni and Au/Ni show close to half metallic state. The magnetic moment of interface Ni is significantly suppressed in the presence of Au adlayer, whereas the magnetic of inner layers are not changed.

It has been observed that the BCC Ni has always in-plane magnetization until 11ML thickness. Very interestingly the Au/Ni manifests thickness dependent spin reorientation transition according to the Au coverage, but there is no consistent trend.

The calculated XAS and XMCD show well separated L edge single peak feature and this can be easily understood from the simple unoccupied DOS as shown.

Since this is the first theoretical report on the thickness dependent SRT in ultrathin BCC Ni film, we hope that the results will stimulate experimental verification.

Reference.

[1]L. H. Tomas, Proc. Camb. Phil. Soc. 23. 542(1926)

[2] E. Fermi, Z, Phys. 48,73 (1928).

[3] P. A. M. Dirac, Proc. Camb. Phil. Soc. 26, 376 (1930).

[4] P. Hohenberg and W. Kohn, Phys. Rev. 136, B 864 (1964).

[5] W. Kohn and L. J. Sham, Phys. Rev. 140, A1133 (1965).

[6] L. Hedin and S.J.Lundqvist , Phys. (France) 33, C3-73 (1972).

[7] J. von Barth and L. Hedin, J. Phys. C 5, 1629 (1972).

[8] O. Gunnarsson, B.I.Lundqvist, and Lundqvist, Solid State Commun. 11 149 (1972).

[9] A. D. Becke, Phys. Rev. A 38, 3098 (1988).

[10] J. P. Perdew and Y. Wang, Phys. Rev. B 45, 13244 (1992).

[11] M. Weinert, E. Wimmer, and A.J.Freeman, Phys. Rev. B 26, 4571 (1982).

[12] 홍순철, 이재일, “표면, 계면, 박막 자성에 대한 전자 구조 이론”, 한국자기학회지 Vol 5, No 4, 315 (1995).

[13] T. Dietl, H. Ohno, F. Matsukura, J. Cibert, and D. Ferrand, Science 287, 1019(2000).

[14] T.W.G. Wyckoff, Crystal Structures, Vol. 1, 2nd Edition, Wiley, New York, 1986, p.112.

[15]G.A. Prinz,Phys. Rev.Lett. 54, 1051 (1985).

[16]D. Qian ,X.F.Jin, J.Barthel, M.Klaua, and J.Kirschner, Phys. Rev. Lett.87 , 227204 (2001)

[17]Y.Tsunoda, J.Phys. Condens .Mater. 1 , 10427, (1989)

[18]V. L. Moruzzi, Phys. Rev.Lett. 57, 2211(1986)

[19]V. L. Moruzzi, P. M. Marcus, and K.Schwarz, Phys. Rev. B. 34, 1784(1986)

[20] E.Wimmer,H.Krakauer, M.Weinert, and A.J.Freeman,Phys.Rev.B 24, 864(1981).

[21]M.Weinert, E. Wimmer, and A.J. Freeman, Phys. Rev.B 26, 4571(1982)

[22]M.Weinert, J. Math. Phys. 2, 2433 (1981).

[23]D.D. Koelling and B.N.Haon, J.Phys.C :Solid State Phys. 10,3107 (1997)

[24]J.P.Perdew, K.Burke, and M.Ernzerhof, Phys.Rev.Lett. 77, 3865 (1996)

[25]B.Heinrich, S.T.Purcell,J.R.Dutcher,K.B.Urquhart,J.F.Cochran, and A.S.Arrot, Phys. Rev.B. 38, 12879.

[26] Z.Q.Wang, Y.S.Li. F. Jona and P.M.Marcus, Solid. State. Commun. 61.623(1987)

[27] A.C. Bland, R.D.Bateson, A.D.Johnson,B.Heinrich, Z. Celinski, and H.J.Lauter, J.Magn.Magn. Mater.93,331 (1991).

[28]o Lin ,M.M. Schwickert, M.A. Tomaz, H. Chen, and G.R.Harp, Phys.Rev.B 59,13911 (1999).

[29]C.S .Tian, D.Qian, D.Wu, R.H. He, Y.Z. Wu, W.X .Tang, L.F. Yin, Y.S.Shi, G.S.Dong, and X.F.Jin, Phys.Rev. Lett.94,137210(2005).

[30]W.X.Tang, D.Qian, D.Wu, Y.Z. Wu, G.S.Dong, X.F. Jin, S.M. Chen,,X.M. Jiang, X.X.Zhang, and Z.Zhang, J.Magn.Mater.240,404(2002).

[31]Sergi Khmelvski and Peter Mphn, Phys.Rev.B 75, 012411(2007).

[32]C.Etz, A.Vernes, L.Szunyogh, and P.Weinberger, Phys.Rev.B 77,064420(2008)

[33] G.Y.Guo and H.H.Wang, Chin. J.Phys. (Taipei), 38, 949 (2000).

[34]M. Weinert, R.E. Watson and J.W. Davenport, Phys. Rev. B. 32, 2115 (1985),

[35]X.D. Wang, D.S. Wang, R. and A.J. Freeman, J.Magn. Magn. Mat., 159337 (1996)

[36]G.H.O Daalderop, P.J. Kelly, and M.F.H. Schuurmans, Phys. Rev. B41,11919(1990); Phys. Rev. B50, 9989 (1994)

[37]R.H. Victora and J.M. MacLaren, Phys. Rev. B45,11583 (1993); J.Appl.Phys., 73, 6415 (1993); IEEE Trans. Mag.,29,3034 (1993).

[38]D.S. Wang, R.Wu and A.J. Freeman, Phys. Rev. Lett., 70.869 (1993)

[39]D.S. Wang, R.Wu and A.J. Freeman, J.Magn.Mang.Mat., 129,237(1994)

[40] Lieping Zhong, Miyoung Kim, X.D.Wang and A.J.Freeman, Phys. Rev. B53,9770 (1996)

[41] X.D. Wang, R.Wu, D.S.Wang and A.J.Freeman, Phys .Rev.B54. 61 91996)

[42]A.B.Shick, D.L.Novikov and A.J.Freeman, Phys. Rev. B 56, R14259 (1997).

[43]X.D.Wang,R.Q. Wu, D.S Wang A.J. Freeman, Phys. Rev.B 54,61 (1996)

[44]Jisang Hong, R.Q. Wu, J.Lindner, E. Kosubek, and K.Baberschke, Phys .Rev.Lett. 92, 147202(2004)

[45]G.Van der Laan, J.Phys : Condens. Mater. 10, 3239 (1998).

[46]I.Galanakis, M.Alouani. and H.Dreysse, Phys. Rev. B 62, 6475(2000).

[47]Till Burkert, Lars Nordstrom, Olle Eriksson, and Olle Heinonen ,Phys.Rev. Lett. 93 , 027203 (2004).

[48]S.Doniach and M.Sunfic, J.Phys. C3, 285 (1970)

감사의 말

2년전 이맘때가 엊그제 같은데, 벌써 졸업이라니요. 시간은 저를 기다려주지 않나봅니다. 어느덧 시간이 지나 이렇게 졸업을 하게 되지만 마음한구석은 꺼림칙합니다. 석사2년 동안 너무 부족했던 것 같고 졸업논문 또한 열심히 했지만 부족한 부분이 왜 이렇게도 많은지 모르겠네요. 하지만 빛나는 졸업장을 받을 수 있는 것은 많은 분들의 도움덕분입니다. 하여, 그분들께 감사의 말을 글로 대신 전하고자 합니다.

먼저, 저의 지도교수님이신 홍지상 교수님께 감사의 말을 전합니다. 교수님의 가르침으로 여기까지 올수 있었습니다. 어떠한 글도 감사의 말을 대신 할 수 없을것입니다. 교수님을 만나서, 교수님이 저의 지도교수님이라서 항상 감사하는 마음으로 지내고 있습니다. 황찬용박사님, 대전에 있을 동안 제가 좀 더 잘했다면 싶습니다. 감사하고, 항상 죄송합니다. 문병기 교수님, 교수님의 말씀은 저를 한번 더 생각하게 합니다. 앞으로도 많은 지도 부탁드립니다. 감사합니다. ((또한, 항상 걱정해주신 김무준교수님, 졸업논문 쓴다고 격려를 아끼지 않으셨던 김선일교수님, 학부때 고마움을 다 표하지 못했던 최병춘교수님, 정중현교수님께도 감사의 말은 전합니다.)) 석사과정동안 많은 지도 해주셨던 물리학과 교수님들께, 이도현 박사님, 김효진 교수님께도 감사의 말 전합니다.
너무 감사한 분들이 많은 것 같습니다. 항상 저에게 힘이 되어주는 나노자성체이론실험실원 세원선배, 혜숙이, 용록이, 수환이, 재율아 항상 고맙고 같은 실험실이라서 행복해. 동유선배! 졸업발표 할 때 나보다 더 긴장하시고 신경 써 주셔서 감사해요! 현경선배 종원선배 저에겐 두 분이 언제나 따뜻한 그 무엇입니다. 고맙습니다. 먼저 졸업한 희진이에게도 고마움을 전합니다.

마지막으로 부모님, 이쁜 경림언니, 말썽꾸러기 동규! 특히 맘고생이 제일 심하셨던 엄마.. 사랑해요. 고맙습니다!!
더욱 열심히 하겠습니다. 모두 행복하세요!